




cGAS is activated by DNA in a length-dependent manner

Stefanie Luecke¹, Andreas Holleufer², Maria H Christensen¹, Kasper L Jønsson¹, Gerardo A Boni¹, Lambert K Sørensen³, Mogens Johannsen³ , Martin R Jakobsen¹, Rune Hartmann²  & Søren R Paludan^{1,*} 

Abstract

Cytosolic DNA stimulates innate immune responses, including type I interferons (IFN), which have antiviral and immunomodulatory activities. Cyclic GMP-AMP synthase (cGAS) recognizes cytoplasmic DNA and signals via STING to induce IFN production. Despite the importance of DNA in innate immunity, the nature of the DNA that stimulates IFN production is not well described. Using low DNA concentrations, we show that dsDNA induces IFN in a length-dependent manner. This is observed over a wide length-span of DNA, ranging from the minimal stimulatory length to several kilobases, and is fully dependent on cGAS irrespective of DNA length. Importantly, *in vitro* studies reveal that long DNA activates recombinant human cGAS more efficiently than short DNA, showing that length-dependent DNA recognition is an intrinsic property of cGAS independent of accessory proteins. Collectively, this work identifies long DNA as the molecular entity stimulating the cGAS pathway upon cytosolic DNA challenge such as viral infections.

Keywords cGAS; DNA sensing; interferon; length dependence; STING

Subject Categories Immunology; Microbiology, Virology & Host Pathogen Interaction; Signal Transduction

DOI 10.15252/embr.201744017 | Received 2 February 2017 | Revised 14 July 2017 | Accepted 18 July 2017 | Published online 10 August 2017

EMBO Reports (2017) 18: 1707–1715

See also: **MP Gantier** (October 2017)

Introduction

Efficient activation of anti-microbial activity upon exposure to pathogens, while avoiding improper immune activation under homeostatic conditions, is one of the main functions of the innate immune system. Nucleic acids in the cytosol, both DNA and RNA, are potent activators of the IFN (interferon) response [1–3]. Pathogen-derived RNA is sensed by RIG-I (retinoic

acid-inducible gene 1) and MDA5 (melanoma differentiation-associated protein 5), while the main cytosolic DNA sensor is cyclic GMP-AMP (cGAMP) synthase (cGAS) [4,5]. Upon DNA binding, cGAS synthesizes the cyclic dinucleotide 2'3'-cGAMP, which acts as a secondary messenger binding to the signaling adaptor STING (stimulator of interferon genes) [6,7]. cGAMP-binding to STING leads to activation of the kinase TBK1 (TANK binding kinase 1), which uses STING as a scaffold to phosphorylate and activate the transcription factor IRF3 (interferon regulatory factor 3), thus eventually inducing IFN expression [8]. Other intracellular proteins have been suggested to act as innate DNA receptors, such as IFI16, which is now thought to be a co-factor for STING-dependent DNA sensing in human cells [9,10].

Clearly defining the molecular nature of the immunostimulatory nucleic acids is essential for understanding how cells identify danger signals. RIG-I recognizes short dsRNAs (> 19 bp) with 5'-triphosphorylated blunt ends, while MDA5 shows a strong length-dependency of signaling, requiring dsRNAs larger than 1,000 bp for efficient signaling [11]. Recognition of dsDNA by cGAS is largely sequence-independent, and cGAS has a preference for B-form DNA [5,12]. The IFN response to cytosolic DNA was shown to be length-dependent at short DNA lengths. Minimally, 20–40 bp are needed for immune activation, depending on the species and cell type, although this length requirement can be lowered to 12 bp through the presence of G-overhangs [13–16]. Previous studies concluded that the optimum length for an efficient innate response to cytosolic DNA is reached already at 45–70 bp [2,13,14]. However, these studies typically used DNA concentrations of at or above 1 µg/ml, which is in sharp contrast to the much lower amounts of DNA reaching the cytosol during an infection. For example, infection with herpes simplex virus 1 (HSV-1), which has a genome of 152 kilobases, in a typical experimental setup would only lead to delivery of 17 ng viral DNA/1 million cells. In addition, microbial genomes are much longer than the DNA used in these studies.

Therefore, we systematically investigate the length-dependency of DNA-induced type I IFN expression for longer DNA, using low DNA concentrations in order to model an infection in a physiological context more closely.

¹ Department of Biomedicine, Aarhus University, Aarhus, Denmark

² Department of Molecular Biology and Genetics, Aarhus University, Aarhus, Denmark

³ Department of Forensic Medicine, Aarhus University Hospital, Aarhus, Denmark

*Corresponding author. Tel: +45 87167843; E-mail: srp@biomed.au.dk

Results and Discussion

The type I IFN response to dsDNA is length-dependent at low DNA concentration

In order to investigate the length-dependency of the innate immune response to dsDNA, we first generated dsDNA molecules ranging from 88 to 4,003 bp by PCR amplification. The absence of contaminating nucleic acid species outside the intended size ranges was confirmed by high-sensitivity automated gel electrophoresis (Fig EV1A). DNA concentrations of the stocks were determined by spectrophotometric concentration determination and confirmed by visual examination of agarose gels (Fig EV1B). When the DNA was delivered to human macrophage-like cells (PMA-differentiated THP-1 cells) by Lipofectamine 2000 transfection at high DNA concentration (1.67 µg/ml), no difference in the amount of secreted type I IFN was visible across the range of DNA sizes from 88 to 4,003 bp (Fig 1A). However, using lower DNA concentration (0.167 µg/ml), we saw striking length-dependency of the type I IFN response, with the longer the DNA stimulating more strongly (Fig 1A). By lowering the DNA concentration even further, we observed that long DNA molecules (2,027 bp, 4,003 bp) are stimulatory at concentrations as low as 0.0167 µg/ml (Fig 1B). We confirmed this by measuring IFNβ mRNA levels by RT-qPCR (Fig EV1C and D). The DNA length-dependent type I IFN response was not limited to the THP-1 cell line, but was also seen in human foreskin fibroblasts (HFF) and in primary human peripheral blood mononuclear cells (PBMCs) (Fig 1C and D). Transfection of THP-1 cells using other lipofectamine reagents such as Lipofectamine LTX or Lipofectamine RNAiMAX (the latter optimized for the transfection of short nucleic acids) resulted in similarly DNA length-dependent stimulation (Figs 1E and EV1E). To confirm that this effect is not specific to PCR-generated DNA and independent of sequence, we generated two sets of restriction fragments from the pOET1-OAS3 plasmid, a set from the plasmid backbone ranging from 108 to 4,570 bp (Fig EV2A and C) and a set from the human gene insert (OAS3) ranging from 196 to 3,317 bp (Fig EV2B and C). As these restriction fragments stimulated the IFN response in THP-1 cells more strongly than the PCR products, we chose a low DNA concentration of 0.033 µg/ml for transfection. Both sets of restriction fragments stimulated the IFN response in a length-dependent manner upon

transfection (Fig 1F and G). Thus, type I IFN production induced by cytosolic dsDNA is dependent on the length of the DNA at low DNA concentrations in human cells.

Signaling via the cGAS-STING pathway is DNA length-dependent

In recent years, cGAS has been established as the main IFN-inducing cytosolic DNA sensor [17]. To confirm that the IFN production seen here is indeed due to activation of the cGAS-STING pathway, we tested the response to dsDNA of various length in both STING- and cGAS-deficient PMA-differentiated THP-1 cells (Fig EV3A, [18]). While type I IFN expression was induced in control cells in the expected length-dependent manner, none of the DNA lengths could stimulate any response in STING- or cGAS-deficient cells (Fig 2A and B). These results from the type I IFN bioassay were confirmed on IFNβ mRNA level by RT-qPCR (Fig EV3B and C). Therefore, the length-dependent DNA sensing studied here is strictly cGAS-STING dependent.

Next, we investigated at which step in the signaling pathway upstream of IFN expression the length-dependent activation was detectable. First, we analyzed levels of phosphorylated TBK1. As seen by Western blotting, transfection with short, medium, and long DNA led to phosphorylation of TBK1 in a length-dependent manner, with the long DNA inducing the strongest TBK1 phosphorylation, while total TBK1 protein levels were equal between transfected and untransfected cells (Fig 2C). We next investigated levels of dimerization and S366 phosphorylation of STING, which both indicate STING activation [8,18]. Similar to pTBK1, levels of dimerization and S366 phosphorylation of STING increased with the length of the transfected DNA (Fig 2D and E). Finally, we evaluated the accumulation of cGAMP in DNA-transfected cells using LC-MS/MS (liquid chromatography tandem mass spectrometry). Cells stimulated with long DNA (4,003 bp) produced more cGAMP than cells transfected with short DNA (94 bp), while mock-transfected cells did not produce any measurable cGAMP (Fig 2F). Thus, the length-dependency of DNA-induced IFN production must occur at the level of DNA binding, cGAS activation, or cGAMP stability.

The above experiments were repeated using the high DNA concentration (1.67 µg/ml). Under these conditions, cGAMP production, STING dimerization, and TBK1 phosphorylation

Figure 1. The cytokine response to dsDNA is length-dependent at low DNA concentration in human cells.

- A Type I IFN levels in supernatants from PMA-differentiated THP-1 cells transfected with Lipofectamine 2000 with PCR-derived dsDNA of indicated lengths at 1.67 µg/ml or 0.167 µg/ml for 12 h, measured by bioassay.
- B Type I IFN levels in supernatants from PMA-differentiated THP-1 cells transfected with PCR-derived dsDNA of indicated lengths at 0.0167 µg/ml for 12 h, measured by bioassay.
- C Type I IFN levels in supernatants from HFFs transfected with PCR-derived dsDNA of indicated lengths at 0.167 µg/ml for 12 h, measured by bioassay.
- D Type I IFN levels in supernatants from PBMCs transfected with PCR-derived dsDNA of indicated lengths at 0.167 µg/ml for 12 h, measured by bioassay.
- E Type I IFN levels in supernatants from PMA-differentiated THP-1 cells transfected with Lipofectamine LTX with PCR-derived dsDNA of indicated lengths at 0.167 µg/ml for 12 h, measured by bioassay.
- F Type I IFN levels in supernatants from PMA-differentiated THP-1 cells transfected with plasmid backbone-derived restriction fragments of indicated lengths at 0.033 µg/ml for 12 h, measured by bioassay.
- G Type I IFN levels in supernatants from PMA-differentiated THP-1 cells transfected with human gene insert-derived restriction fragments of indicated lengths at 0.033 µg/ml for 12 h, measured by bioassay.

Data information: Data are represented as mean ± SD of biological triplicates from one experiment. Statistical significance was analyzed using one-way ANOVA. ns non-significant, **P* < 0.05, ***P* < 0.01, ****P* < 0.001, *****P* < 0.0001. The experiments were performed three times (A–C, E–G) or one time each with cells from two donors (D). Broken horizontal lines indicate detection limit of assays. See also Figs EV1 and EV2.

remained length-dependent (Fig EV3D–F), indicating that the saturation of the IFN-inducing pathway, which results in the lack of length-dependency at the level of IFN production at high DNA

concentration, must occur downstream of TBK1 phosphorylation, for example, at the level of IRF3 activity or IFN-receptor feedback signaling.

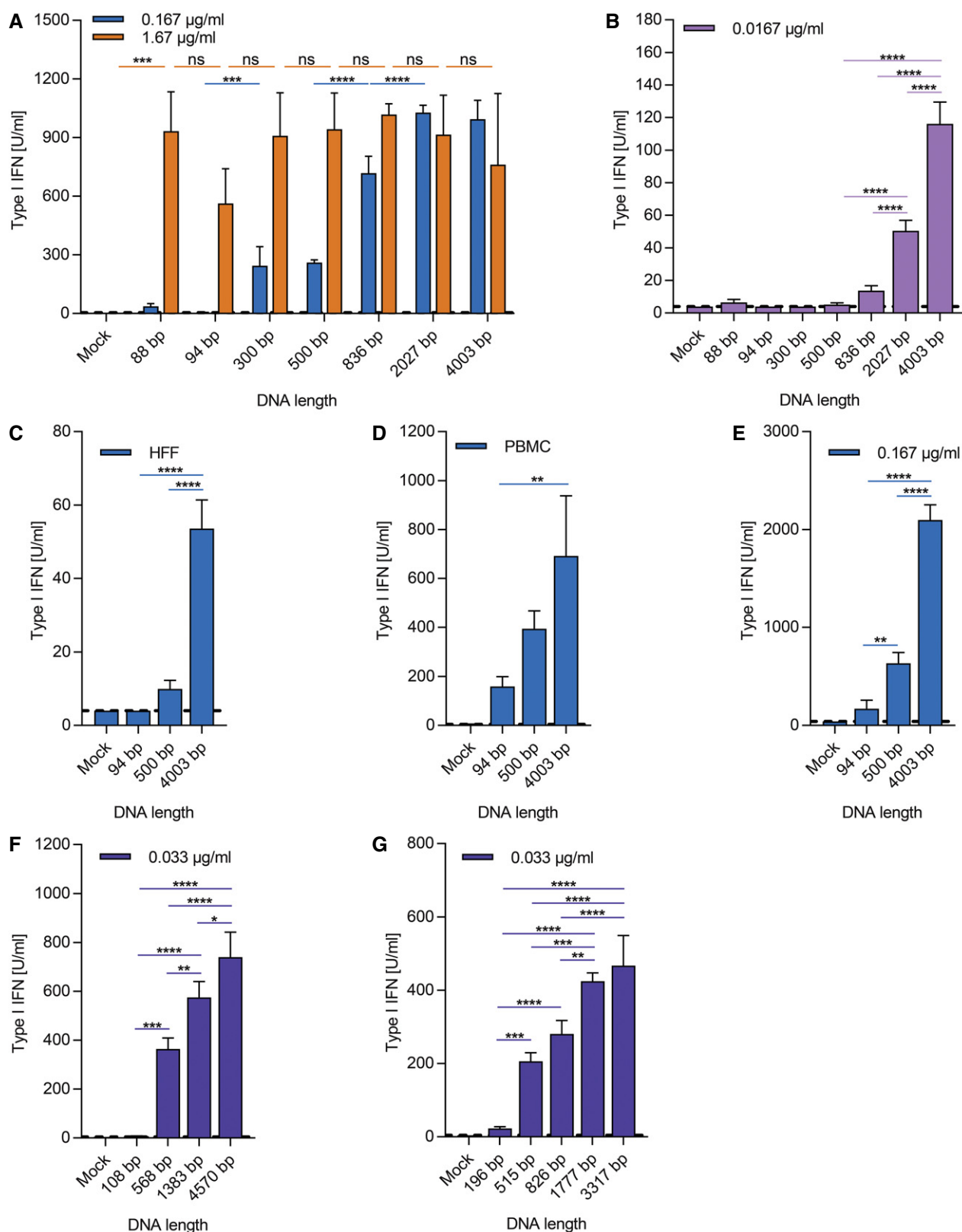


Figure 1.

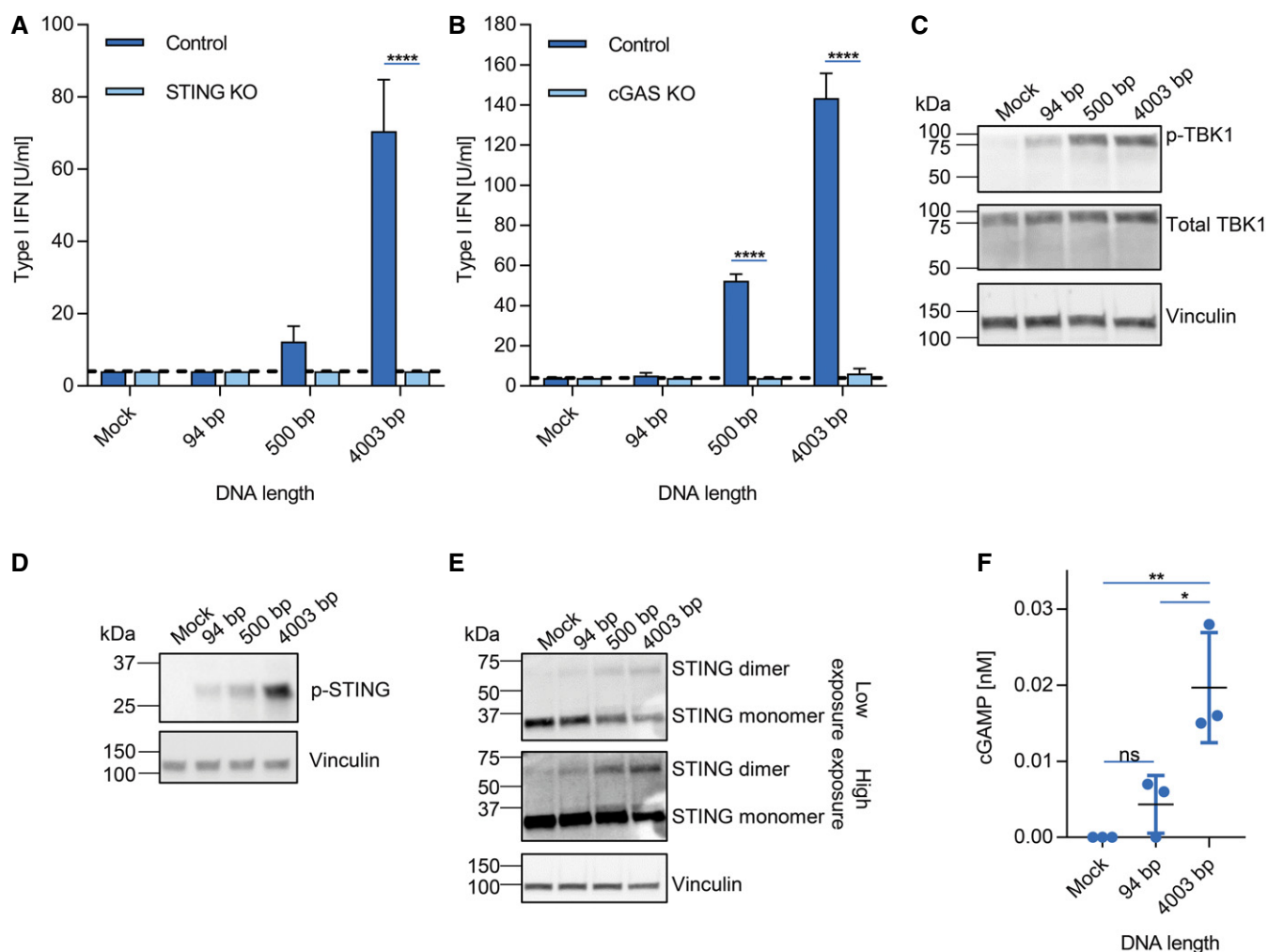


Figure 2. Signaling via the cGAS-STING pathway is DNA length-dependent.

A, B Type I IFN levels in supernatants from PMA-differentiated THP-1 cells deficient in STING (A) or cGAS (B) transfected with PCR-derived dsDNA of indicated lengths at 0.167 $\mu\text{g}/\text{ml}$ for 12 h, measured by bioassay.

C–E Levels of phosphorylated TBK1 (p-TBK1) (C), phosphorylated STING (D), and dimerized STING protein (E) in PMA-differentiated THP-1 transfected with PCR-derived dsDNA of indicated lengths at 0.167 $\mu\text{g}/\text{ml}$ for 2 h. Proteins in cell lysate were separated by SDS–PAGE under reducing (C, D) or non-reducing (E) conditions. After Western blotting, membranes were probed with anti-TBK1, anti-p-TBK1 (C), anti-p-STING (S366) (D), anti-STING (E), and anti-vinculin as a loading control.

F cGAMP levels in PMA-differentiated THP-1 cells transfected with PCR-derived dsDNA of indicated lengths at 0.167 $\mu\text{g}/\text{ml}$ for 8 h, determined by semi-quantitative LC–MS/MS analysis.

Data information: Data are represented as mean \pm SD of biological triplicates from one experiment. Statistical significance was using one-way ANOVA. ns non-significant, * $P < 0.05$, ** $P < 0.01$, **** $P < 0.0001$. Broken horizontal lines indicate detection limit of assay (A, B). The experiments were performed three times (A–E) or two times (F). See also Fig EV3.

Source data are available online for this figure.

Length-dependent IFN induction is not due to differential transfection efficiency or TREX1 sensitivity, nor due to involvement of IFI16 as co-factor

To test the influence of transfection efficiency on the length-dependency, we quantified the amount of DNA recovered from lysates of PMA-differentiated THP-1 cells transfected with short (94 bp) or long DNA (4,003 bp) at 30 min and 3 h after transfection using quantitative real-time PCR. The long DNA was not transfected with a higher efficiency than the short one; rather, there was a trend for the short DNA being transfected better than the long DNAs (Fig 3A).

Differences in transfection efficiency are therefore highly unlikely to be responsible for the stronger IFN response induced by long DNA.

TREX1 is a cytosolic exonuclease essential for keeping the cytoplasm clear of DNA and defective TREX1 leads to IFN-driven pathology [19,20]. Another possible explanation for the length-dependency could be that TREX1 digests short DNA species more efficiently, since they offer more ends per weight unit for the exonuclease to start degradation. To investigate this, we transfected control or TREX1-deficient cells (Fig EV3A) with short, medium, or long DNA. However, both TREX1-deficient cells and control cells show length-dependency of the type I IFN response, with

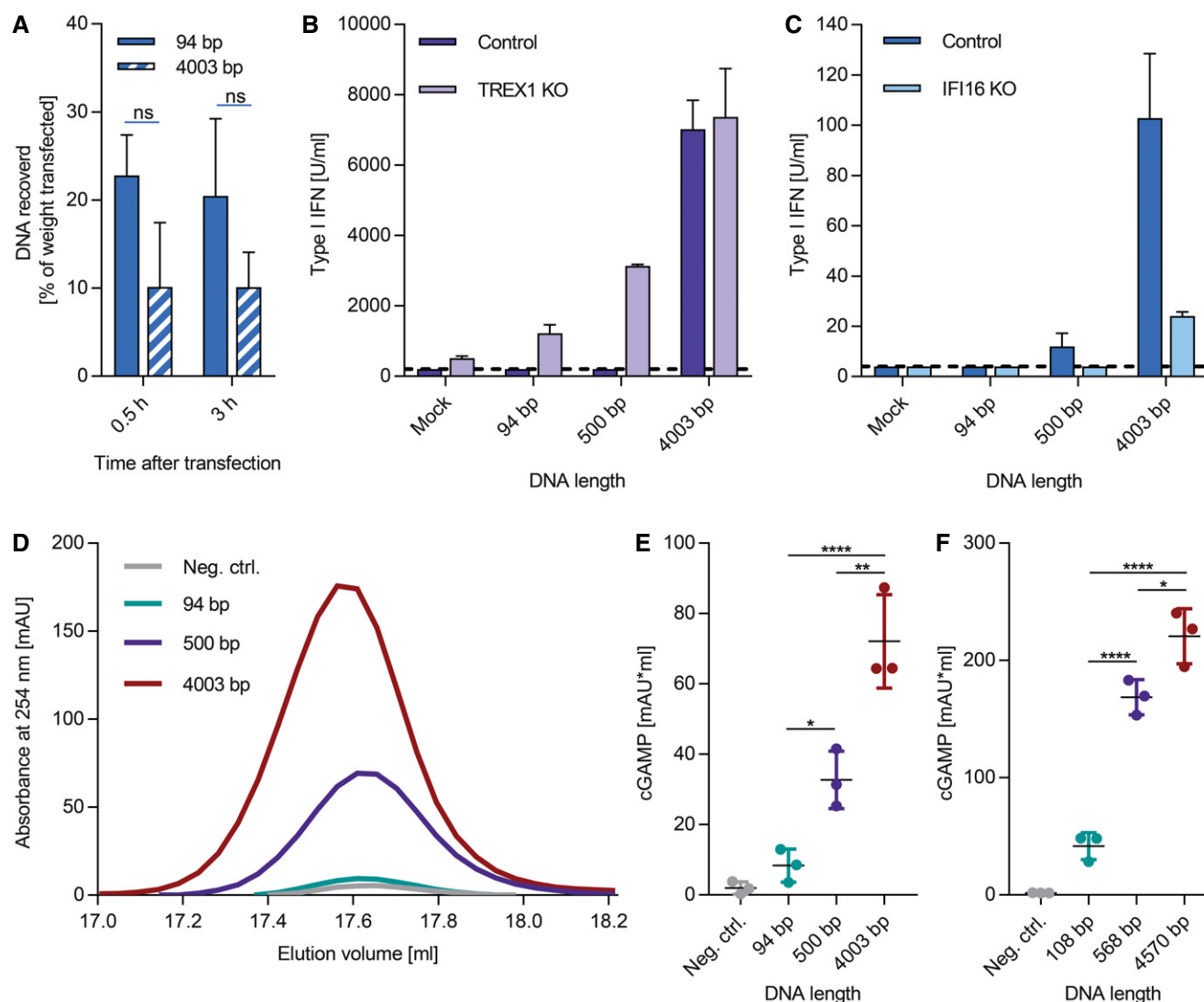


Figure 3. The length-dependent stimulation of cGAMP production by DNA is explained by cGAS alone.

- A** Transfection efficiency of short and long DNA measured as DNA recovered from cell lysates. PMA-differentiated THP-1 cells were transfected with 0.167 $\mu\text{g}/\text{ml}$ PCR-derived DNA of 94 and 4,003 bp. Cells were lysed 0.5 and 3 h later, and the DNA copy number in diluted lysate was determined by qPCR using primers for an 88-bp amplicon common to both fragments. The weight of recovered DNA was calculated and expressed as percentage of input DNA.
- B, C** Type I IFN levels in supernatants from PMA-differentiated THP-1 cells deficient in TREX1 (B) or IFI16 (C) transfected with PCR-derived dsDNA of indicated lengths at 0.033 $\mu\text{g}/\text{ml}$ (B) or 0.167 $\mu\text{g}/\text{ml}$ (C) for 12 h, measured by bioassay. A lower DNA concentration was used for experiments with TREX1-deficient cells than for the other transfection experiments since these commercial cells are stimulated very strongly by DNA.
- D** *In vitro* cGAMP production by h-cGAS. 100 nM recombinant human cGAS ($\Delta\text{N-ter}$) was incubated with PCR-derived dsDNA of indicated lengths at 1 ng/ μl in the presence of ATP and GTP for 2 h. Resulting cGAMP was detected on an anion exchange chromatogram obtained at 254 nm. Absorbance values from one representative experiment are shown.
- E** Area under curves for *in vitro* cGAMP production assay using PCR-derived dsDNA (as in D), representative of amount of cGAMP generated *in vitro*.
- F** Area under curves for *in vitro* cGAMP production assay using plasmid backbone-derived restriction fragments (1 ng/ μl), representative of amount of cGAMP generated *in vitro*.

Data information: Data are represented as mean \pm SD of biological triplicates in one experiment (A–C) or as mean \pm SD of three independent experiments (E, F). Statistical significance was analyzed using one-way ANOVA. ns non-significant, * $P < 0.05$, ** $P < 0.01$, **** $P < 0.0001$. The experiments were performed three times. Broken horizontal lines indicate detection limit of assay (B, C). See also Fig EV4.

TREX1-deficient cells showing an overall increased level of IFN production in response to DNA transfection (Fig 3B). These data from the IFN bioassay were confirmed on the level of IFN β mRNA by qPCR (Fig EV4A), thus eliminating differential sensitivity to TREX1 as the explanation for the length-dependent IFN induction by DNA.

IFI16 (interferon-inducible protein 16), originally suggested as an IFN-stimulating intracellular DNA sensor of its own accord [14], is now considered a co-factor for STING-dependent DNA sensing in specific human cell types [9,10]. DNA binding by IFI16 has been shown to be cooperatively length-dependent [21]. Therefore, we

hypothesized that the involvement of IFI16 in cGAS-dependent DNA sensing might play a role in the observed length-dependency of the resulting IFN response. In order to test this, cells deficient for IFI16 (Fig EV3A, [9]) were transfected with short, medium, and long DNA at a concentration of 0.167 $\mu\text{g}/\text{ml}$. Although the type I IFN response to DNA was impaired in IFI16-deficient cells, the length dependency of the IFN response was still clearly visible in IFI16-deficient cells (Figs 3C and EV4B). This indicates that IFI16 is not responsible for the length-dependency of the IFN response to DNA stimulation.

cGAMP production by recombinant h-cGAS is DNA length-dependent

To test whether cGAS produces cGAMP in a DNA length-dependent manner in the absence of cellular factors, we performed an *in vitro* cGAS activity assay. We chose to perform the *in vitro* assay at the lowest DNA concentration yielding a reliable measurement of cGAS activity in order to model the cellular situation. 100 nM recombinant human cGAS ($\Delta\text{N-ter}$) was incubated with 1 ng/ μl DNA of varying lengths, and resulting cGAMP levels were quantified by ion exchange chromatography measuring area under peak (absorbance measurement at 254 nm) (Fig 3D and E). While short PCR-derived DNA activated cGAS to synthesize a measurable, but very low amount of cGAMP, incubation with medium DNA resulted in intermediate cGAMP levels, while long DNA induced synthesis of a higher amount of cGAMP. The plasmid backbone-derived restriction fragments activated cGAS in a similarly length-dependent manner (Fig 3F). For full chromatograms, see Fig EV4C and D, and for control elutions of commercial ATP, GTP, and cGAMP, see Fig EV4E. These experiments demonstrate that the DNA length-dependent accumulation of cGAMP upon DNA stimulation is due to intrinsic properties of cGAS and independent of cellular co-factors.

Here, we show that cGAS is activated to produce cGAMP by DNA in a length-dependent manner that is especially visible at low DNA concentrations. cGAS is essential for the immune response to many intracellular bacteria and viruses [22–26]. Common to these microbes is that their genomes are much longer than the short DNA species that accumulate in the cytoplasm in the absence of infection [27]. For instance, *Listeria monocytogenes* has a genome of 2.94 Mb and HSV-1 has a genome of 152 kb [28,29]. Thus, during infection with an intracellular DNA pathogen, cGAS is challenged with the task of reliably and rapidly detecting long DNA species present at low abundance, without reacting to self-DNA. Our study suggests that cGAS may achieve this distinction by length-dependent recognition of DNA. Long DNA molecules overcome a requirement for high DNA concentrations, meaning that long DNA molecules can efficiently induce IFN expression at very low concentrations, whereas short DNA species need to be present at high concentrations to induce a strong response. The length threshold for an effective immune response increases from 45 to 70 bp at or above 1 $\mu\text{g}/\text{ml}$ [2,13,14] to 300–500 bp at 0.167 $\mu\text{g}/\text{ml}$ to 800–2,000 bp at 0.017 $\mu\text{g}/\text{ml}$. The use of high concentrations of cGAS and DNA, resulting in substrate exhaustion, may explain why previous *in vitro* studies have concluded that 20-bp DNA can stimulate recombinant cGAS to produce cGAMP as efficiently as salmon sperm DNA (~1,000 bp in lengths) [30].

The mechanism of length-dependent DNA sensing by cGAS remains to be determined. For other cytosolic DNA sensing proteins such as AIM2 and IFI16, length-dependent DNA binding is based on cooperative oligomerization and filament formation on the DNA [21,31]. Likewise, the length-dependent dsRNA sensor MDA5 forms dimers that oligomerize as helical filaments cooperatively on RNA [32–34]. Murine cGAS is known to interact with DNA as a DNA binding-induced 2:2 dimer, which is important for the activation of cGAS, but it has also been suggested that higher order oligomers may occur [30,35]. It should be noted that our data argue against the previous suggestions that cGAS is activated primarily by the ends of dsDNA [30,36]. In our experiments, there are clearly more dsDNA ends available in the experiments with 94-bp DNA than the experiments with 4,003-bp DNA. Nevertheless, the 4,003-bp DNA is a much more potent activator of cGAS. Moreover, undigested circular plasmid DNA can potentially activate cGAS to synthesize cGAMP *in vitro* (Fig EV4F), arguing against a mandatory role for DNA ends in cGAS activation.

In conclusion, we show that DNA-stimulated production of type I IFN occurs in a DNA length-dependent manner at low concentrations, and this is explained by cGAS being activated by long DNA species under these conditions. In this way, cells are able to stimulate protective immune responses to even low levels of incoming microbial DNA material, without allowing shorter DNAs that may accumulate as a by-product of cell division and DNA repair to evoke pathological immune responses.

Materials and Methods

Cell culture and transfection

The human monocyte-like THP-1 cells were obtained from ATCC (TIB-202). THP-1 cGAS^{-/-}, STING^{-/-}, B2M^{-/-} (used as control for cGAS^{-/-}, STING^{-/-}, and IFI16^{-/-} cells), and IFI16^{-/-} cells were previously generated using CRISPR-Cas9 technology [9,18]. THP-1 Dual KO-TREX1 cells and THP-1 Dual cells (used as control for KO-TREX1 cells) were obtained from InvivoGen. THP-1 cells were maintained in RPMI 1640 medium (Lonza) supplemented with 10% fetal calf serum (Sigma), 2 mM L-glutamine (Sigma-Aldrich) 100 U/ml penicillin, 100 $\mu\text{g}/\text{ml}$ streptomycin (Gibco). Additionally, the medium of the Dual cells was supplemented with 100 $\mu\text{g}/\text{ml}$ Normocin, 10 $\mu\text{g}/\text{ml}$ blasticidin, and 100 $\mu\text{g}/\text{ml}$ Zeocin (InvivoGen). Before experiments, THP-1 cells were differentiated into macrophage-like cells with 150 nM phorbol 12-myristate 13-acetate (PMA) (Sigma).

PBMCs were isolated from healthy blood donors (Blood Bank, Aarhus University Hospital) by Ficoll–Paque density gradient and seeded in RPMI 1640 supplemented with 10% fetal calf serum. Human foreskin fibroblasts (HFFs, ATCC-SCRC-1041) were maintained in DMEM (Lonza), supplemented with 15% fetal calf serum, 2 mM L-glutamine, 100 U/ml penicillin, and 100 $\mu\text{g}/\text{ml}$ streptomycin.

HEK-Blue IFN α/β cells (InvivoGen) were maintained in DMEM (Lonza), supplemented with 10% fetal calf serum, 2 mM L-glutamine, 100 U/ml penicillin, 100 $\mu\text{g}/\text{ml}$ streptomycin, 100 $\mu\text{g}/\text{ml}$ Normocin, 30 $\mu\text{g}/\text{ml}$ blasticidin, and 100 $\mu\text{g}/\text{ml}$ Zeocin. Cells were cultured at 37°C in a humidified atmosphere with 5% CO₂.

Cells were transfected with dsDNA of indicated lengths and concentrations using Lipofectamine 2000, Lipofectamine LTX, or Lipofectamine RNAiMAX (Invitrogen) according to the manufacturer's instruction with 30 μ l lipofectamine/ml transfection mixture. Lipofectamine 2000 was used unless indicated otherwise. "Mock" transfection indicates lipofectamine treatment without DNA.

Preparation of PCR-derived dsDNA

Double-stranded DNA molecules were generated by PCR amplification with DreamTaq polymerase (Thermo Scientific) using pcDNA3.1 as a template. One forward primer was used for all PCRs and varying reverse primers resulted in different length amplicons. The PCR products were purified using GeneJET PCR purification kit (Thermo Scientific). The size specificity of the PCR products was verified by automated gel electrophoresis on the Fragment Analyzer (AATI) using the High Sensitivity NGS Fragment Analysis kit (DNF-474, AATI) according to the manufacturer's instructions. The DNA stocks (100 ng/ μ l) used for transfection of cells were additionally visualized by agarose gel electrophoresis (1.5%).

The following primers were used for generation of dsDNA molecules from the pcDNA3.1 vector template:

Forward primer: 5'-CGATGTACGGGCCAGATATACG-3'
 Reverse primer 88 bp: 5'-TGGGCTATGAACTAATGACCCC-3'
 Reverse primer 94 bp: 5'-CATATATGGGCTATGAACTAATGACC-3'
 Reverse primer 300 bp: 5'-TCAATAGGGGGCGTACTTGGCA-3'
 Reverse primer 500 bp: 5'-AACTCCATTGACGTCAATGGGG-3'
 Reverse primer 836 bp: 5'-GCAACTAGAAGGCACAGTCG-3'
 Reverse primer 2,027 bp: 5'-CATCAGAGCAGCCGATTGTC-3'
 Reverse primer 4,003 bp: 5'-CGCTACCAGCGGTGGTTTGT-3'

Preparation of restriction digestion-derived dsDNA

Restriction fragments were generated by restriction digestion of the pOET1-OAS3 plasmid [37]. The set of human gene insert (OAS3)-derived fragments was generated by digestion with NcoI (3,317 bp) and by double digestion with NcoI and XhoI (196, 515, 826, 1,777 bp). The set of plasmid backbone-derived fragments was generated by digestion with VspI (108, 568, 1,383 bp) and with NcoI (4,570 bp). After restriction digestion, fragments were gel-isolated. The size specificity of the restriction fragments was verified by automated gel electrophoresis on the Fragment Analyzer (AATI) using the High Sensitivity NGS Fragment Analysis kit (DNF-474, AATI) (OAS3-derived) or using the High Sensitivity Large Fragment 50 kb Analysis kit (DNF-464, AATI) according to the manufacturer's instructions. For experiments using circular DNA, the undigested pOET1-OAS3 plasmid was used. The DNA stocks (30 ng/ μ l) used for transfection of cells were additionally visualized by agarose gel electrophoresis (1.5%).

Type I IFN bioassay

For determination of type I IFN activity in cell supernatant, 1.5×10^5 THP-1 cells, 3×10^4 HFFs, or 1.5×10^6 PBMCs were transfected in 300 μ l culture medium in 48-well plates. 12 h after transfection, the supernatant was harvested. Levels of type I IFN

were determined using HEK-Blue IFN α/β reporter cells, which express SEAP enzyme under the control of ISG54 promoter upon stimulation of the IFNAR, according to the manufacturer's instruction. SEAP levels were quantified by detecting color change of the QUANTI-Blue substrate (Invivogen) at 620 nm on ELx808 (BioTek). Human IFN α (PBL assay science) was used to generate a standard curve.

RT-qPCR

For determination of IFN β mRNA levels, 1.5×10^5 THP-1 cells were transfected in 300 μ l culture medium in 48-well plates. 6 h after transfection, the cells were lysed for total RNA isolation using the High Pure RNA Isolation kit (Roche). IFN β and β -actin (for normalization) levels were measured with the TaqMan RNA-to-Ct 1-step kit (Applied Biosystems) using TaqMan gene expression assays Hs01077958_s1 (IFNB1) and Hs00357333_g1 (ACTB) on the Aria Mx Real Time PCR System.

SYBR qPCR for determination of transfection efficiency

For determination of differences in transfection efficiency between short and long DNA, 1.5×10^5 THP-1 cells were transfected with 50 ng/well DNA of 94 and 4,003 bp in 300 μ l cell culture medium in a 48-well plate. Cells were lysed 0.5 and 3 h after transfection in RNA lysis buffer (Roche). The lysate was diluted 1:100, and the DNA copy number in 2 μ l diluted lysate was determined by qPCR (Brilliant III SYBR Master Mix, Agilent) using primers for the 88-bp amplicon common to both fragments. The weight of recovered DNA was calculated and expressed as percentage of input DNA.

Western blotting

For Western blotting experiments, 3×10^5 THP-1 cells were transfected with 0.167 μ g/ml or 1.67 μ g/ml DNA in 600 μ l cell culture medium in 24-well plates. 2 h after transfection, cells were lysed in 200 μ l RIPA buffer (ThermoScientific) complemented with protease inhibitor (Roche), phosphatase inhibitor, and benzonase (Sigma). Lysates were cleared of nuclei by centrifugation for 10 min at 14,000 g. Samples were prepared by addition of XT sample buffer (Bio-Rad) and, only when using reducing conditions, by addition of XT reducing agent (Bio-Rad) and boiling at 95°C. Proteins were separated by SDS-PAGE (Criterion TGX 4–20%, Bio-Rad) and transferred to PVDF membranes using the Trans-Blot Turbo Transfer System (Bio-Rad). Blocking of membranes was carried out in 5% milk for 1 h at room temperature, before incubation with primary antibodies at 4°C for 16 h. Membranes were incubated with HRP-conjugated secondary antibodies (Jackson ImmunoResearch) for 1 h at room temperature and developed using Super Signal West Dura extended duration substrate (ThermoScientific). The following primary antibodies were used: p-TBK1 (CST D52C2), TBK1 (CST D1B4), p-STING (S366) (CST #85735S), STING (CST D2P2F), and vinculin (Sigma V9131). For determination of expression levels of cGAS, STING, IFI16, and TREX1 in deficient PMA-differentiated THP-1 cells, the following primary antibodies were used: cGAS (CST D1D3G), STING (RnD AF6516), IFI16 (sc-8023), and TREX1 (sc-271870).

Quantification of cellular cGAMP levels by LC-MS/MS

3×10^6 THP-1 cells were transfected with 0.167 $\mu\text{g}/\text{ml}$ DNA or 1.67 $\mu\text{g}/\text{ml}$ in 2 ml medium in 6-well plates. 8 h after transfection, cells were lysed in a lysis buffer of 80% methanol, 2% acetic acid, and 18% ddH₂O. cGAMP purification and liquid chromatography tandem mass spectrometry (LC-MS/MS) detection were performed as described previously [9]. To achieve semi-quantitative results, blank samples were spiked with cGAMP to concentrations of 0, 1, and 10 nM and used as external calibrators.

Protein purification

A truncated form of human cGAS was expressed in *E. coli* BL21 (DE3) as a 6xN-His MBP-cGAS [155–522] fusion protein. The expression was induced with 1 mM of isopropyl- β -D-thiogalactoside for 18 h at 18°C. The cells were harvested and lysed by sonication in a buffer containing 300 mM NaCl, 50 mM NaPO₄, 25 mM imidazole, 5 mM β -mercaptoethanol, 10% (v/v) glycerol, 0.1% (v/v) NP-40, pH 8.0. Cleared lysate was incubated with Ni Sepharose TM 6 Fast Flow (GE Healthcare) for 2.5 h at 4°C. The resin was transferred to a gravity flow column and washed twice with 1 M NaCl, 20 mM Tris, 25 mM imidazole, 5 mM β -mercaptoethanol, 10% (v/v) glycerol, pH 7.5. The protein was eluted with 300 mM NaCl, 20 mM Tris, 350 mM imidazole, 5 mM β -mercaptoethanol, 10% (v/v) glycerol, pH 7.5. The eluate was diluted six times with a buffer containing 300 mM NaCl, 20 mM HEPES, 1 mM DTT, 10% (v/v) glycerol, pH 7.5 and incubated with 1 μg of TEV protease per 50 μg of protein. cGAS [155–522] was further purified using a 5 ml HiTrapTM Heparin HP column (GE Healthcare) and eluted with a gradient going from 100% buffer A (50 mM NaCl, 10% glycerol, 20 mM HEPES pH 7.5) to 100% buffer B (2 M NaCl, 10% glycerol, 20 mM HEPES pH 7.5). The eluted cGAS [155–522] was diluted four times to a concentration of 0.66 mg/ml with buffer A, flash-frozen, and stored at -80°C .

In vitro cGAMP synthesis and detection

100 nM recombinant cGAS was incubated with 1 ng/ μl DNA of indicated lengths and indicated origin in a buffer containing 80 mM Tris-HCl, pH 7.5, 200 mM NaCl, 20 μM ZnCl₂, and 20 mM MgCl₂ in the presence of 0.5 mM ATP and 0.5 mM GTP in a total volume of 200 μl for 2 h at 37°C, followed by heat inactivation at 95°C for 10 min. Two independent PCR-derived DNA preparations and one restriction fragment preparation were used for the *in vitro* experiments. The samples were diluted five times in 20 mM Tris pH 7.5. 800 μl of the sample was loaded onto a 1 ml RESOURCE™ Q column (GE Healthcare). The nucleotides were eluted with a gradient starting with 20 mM Tris pH 7.5 reaching 375 mM NaCl (PCR-derived DNA and control elutions) or 300 mM NaCl (restriction-derived DNA) and 20 mM Tris pH 7.5 over 25 column volumes (PCR-derived DNA and control elutions) or 18 column volumes (restriction-derived DNA). The flow was set to 0.5 ml/min. A chromatogram was obtained for absorbance at 254 nm. To quantify the cGAMP peak, the chromatogram peaks were integrated using the software Unicorn 5.10 (GE Healthcare) with default settings.

Statistical analysis

The data are shown as mean \pm SD, either from biological triplicates in one experiment or from three independent experiments, as indicated. The experiments were repeated as indicated. Statistical analysis was performed using the GraphPad Prism 7.02 software. For comparison of multiple groups, statistical significance between experimental groups was determined using ordinary one-way ANOVA. When performing ANOVA, the Brown–Forsythe test was used to exclude significant differences in standard deviations. Tukey's method was used to correct for multiple comparisons when comparing the mean of all the samples with each other and Sidak's method was used when comparing the mean of preselected pairs of samples (e.g., for comparison of control cells with deficient cells).

Expanded View for this article is available online.

Acknowledgements

We thank Kirsten Stadel Petersen (Aarhus University) for technical assistance and Robert-Jan Lebbink (University Medical Center Utrecht) for CRISPR-Cas9 THP-1 cells. This work was funded by the Boehringer Ingelheim Fonds (PhD stipend to S.L.), The Novo Nordisk Foundation (NNF13OC0006211 S.R.P.; NNF15OC0017902, R.H.), The Lundbeck Foundation (R198-2015-171, S.R.P.; R151-2013-14443, M.R.J., K.L.J.), the Danish Council for Independent Research, Medical Research (12-124330, S.R.P.; 4183-00032B, R.H.; 4004-00237, M.R.J., K.L.J.), the Danish Council for Independent Research, Natural Science (4181-00012B, R.H., A.H.), and the Augustinus Fond (M.R.J., K.L.J.).

Author contributions

SL and SRP conceived the idea and designed the experiments. SL, AH, MHC, KLJ, GAB, and LKS performed the experiments. MJ, MRJ, RH, and SRP supervised experiments. SL drafted the manuscript. AH, MRJ, RH, and SRP edited the manuscript. All authors approved the manuscript.

Conflict of interest

The authors declare that they have no conflict of interest.

References

- Diebold SS, Montoya M, Unger H, Alexopoulou L, Roy P, Haswell LE, Al-Shamkhani A, Flavell R, Borrow P, Reis e Sousa C (2003) Viral infection switches non-plasmacytoid dendritic cells into high interferon producers. *Nature* 424: 324–328
- Stetson DB, Medzhitov R (2006) Recognition of cytosolic DNA activates an IRF3-dependent innate immune response. *Immunity* 24: 93–103
- Ishii KJ, Coban C, Kato H, Takahashi K, Torii Y, Takeshita F, Ludwig H, Sutter G, Suzuki K, Hemmi H *et al* (2006) A Toll-like receptor-independent antiviral response induced by double-stranded B-form DNA. *Nat Immunol* 7: 40–48
- Yoneyama M, Kikuchi M, Natsukawa T, Shinobu N, Imaizumi T, Miyagishi M, Taira K, Akira S, Fujita T (2004) The RNA helicase RIG-I has an essential function in double-stranded RNA-induced innate antiviral responses. *Nat Immunol* 5: 730–737
- Sun L, Wu J, Du F, Chen X, Chen ZJ (2013) Cyclic GMP-AMP synthase is a cytosolic DNA sensor that activates the type I interferon pathway. *Science* 339: 786–791

6. Wu J, Sun L, Chen X, Du F, Shi H, Chen C, Chen ZJ (2013) Cyclic GMP-AMP is an endogenous second messenger in innate immune signaling by cytosolic DNA. *Science* 339: 826–830
7. Ablasser A, Goldeck M, Cavlar T, Deimling T, Witte G, Rohl I, Hopfner KP, Ludwig J, Hornung V (2013) cGAS produces a 2'-5'-linked cyclic dinucleotide second messenger that activates STING. *Nature* 498: 380–384
8. Liu S, Cai X, Wu J, Cong Q, Chen X, Li T, Du F, Ren J, Wu YT, Grishin NV et al (2015) Phosphorylation of innate immune adaptor proteins MAVS, STING, and TRIF induces IRF3 activation. *Science* 347: aaa2630
9. Jonsson KL, Laustsen A, Krapp C, Skipper KA, Thavachelvam K, Hotter D, Egedal JH, Kjolby M, Mohammadi P, Prabhakaran T et al (2017) IFI16 is required for DNA sensing in human macrophages by promoting production and function of cGAMP. *Nat Commun* 8: 14391
10. Almine JF, O'Hare CA, Dunphy G, Haga IR, Naik RJ, Atrih A, Connolly DJ, Taylor J, Kelsall IR, Bowie AG et al (2017) IFI16 and cGAS cooperate in the activation of STING during DNA sensing in human keratinocytes. *Nat Commun* 8: 14392
11. Schlee M, Hartmann G (2016) Discriminating self from non-self in nucleic acid sensing. *Nat Rev Immunol* 16: 566–580
12. Civril F, Deimling T, de Oliveira Mann CC, Ablasser A, Moldt M, Witte G, Hornung V, Hopfner KP (2013) Structural mechanism of cytosolic DNA sensing by cGAS. *Nature* 498: 332–337
13. Karayel E, Burckstummer T, Bilban M, Durnberger G, Weitzer S, Martinez J, Superti-Furga G (2009) The TLR-independent DNA recognition pathway in murine macrophages: ligand features and molecular signature. *Eur J Immunol* 39: 1929–1936
14. Unterholzner L, Keating SE, Baran M, Horan KA, Jensen SB, Sharma S, Sirois CM, Jin T, Latz E, Xiao TS et al (2010) IFI16 is an innate immune sensor for intracellular DNA. *Nat Immunol* 11: 997–1004
15. Ablasser A, Bauernfeind F, Hartmann G, Latz E, Fitzgerald KA, Hornung V (2009) RIG-I-dependent sensing of poly(dA:dT) through the induction of an RNA polymerase III-transcribed RNA intermediate. *Nat Immunol* 10: 1065–1072
16. Herzner AM, Hagmann CA, Goldeck M, Wolter S, Kubler K, Wittmann S, Gramberg T, Andreeva L, Hopfner KP, Mertens C et al (2015) Sequence-specific activation of the DNA sensor cGAS by Y-form DNA structures as found in primary HIV-1 cDNA. *Nat Immunol* 16: 1025–1033
17. Paludan SR (2015) Activation and regulation of DNA-driven immune responses. *Microbiol Mol Biol Rev* 79: 225–241
18. Holm CK, Rahbek SH, Gad HH, Bak RO, Jakobsen MR, Jiang Z, Hansen AL, Jensen SK, Sun C, Thomsen MK et al (2016) Influenza A virus targets a cGAS-independent STING pathway that controls enveloped RNA viruses. *Nat Commun* 7: 10680
19. Stetson DB, Ko JS, Heidmann T, Medzhitov R (2008) Trex1 prevents cell-intrinsic initiation of autoimmunity. *Cell* 134: 587–598
20. Crow YJ, Hayward BE, Parmar R, Robins P, Leitch A, Ali M, Black DN, van Bokhoven H, Brunner HG, Hamel BC et al (2006) Mutations in the gene encoding the 3'-5' DNA exonuclease TREX1 cause Aicardi-Goutieres syndrome at the AGS1 locus. *Nat Genet* 38: 917–920
21. Morrone SR, Wang T, Constantoulakis LM, Hooy RM, Delannoy MJ, Sohn J (2014) Cooperative assembly of IFI16 filaments on dsDNA provides insights into host defense strategy. *Proc Natl Acad Sci USA* 111: E62–E71
22. Li XD, Wu J, Gao D, Wang H, Sun L, Chen ZJ (2013) Pivotal roles of cGAS-cGAMP signaling in antiviral defense and immune adjuvant effects. *Science* 341: 1390–1394
23. Schoggins JW, MacDuff DA, Imanaka N, Gainey MD, Shrestha B, Eitson JL, Mar KB, Richardson RB, Ratushny AV, Litvak V et al (2014) Pan-viral specificity of IFN-induced genes reveals new roles for cGAS in innate immunity. *Nature* 505: 691–695
24. Collins AC, Cai H, Li T, Franco LH, Li XD, Nair VR, Scharn CR, Stamm CE, Levine B, Chen ZJ et al (2015) Cyclic GMP-AMP synthase is an innate immune DNA sensor for *Mycobacterium tuberculosis*. *Cell Host Microbe* 17: 820–828
25. Reinert LS, Lopusna K, Winther H, Sun C, Thomsen MK, Nandakumar R, Mogensen TH, Meyer M, Vaegter C, Nyengaard JR et al (2016) Sensing of HSV-1 by the cGAS-STING pathway in microglia orchestrates antiviral defence in the CNS. *Nat Commun* 7: 13348
26. Watson RO, Bell SL, MacDuff DA, Kimmey JM, Diner EJ, Olivas J, Vance RE, Stallings CL, Virgin HW, Cox JS (2015) The cytosolic sensor cGAS detects *Mycobacterium tuberculosis* DNA to induce type I interferons and activate autophagy. *Cell Host Microbe* 17: 811–819
27. Yang YG, Lindahl T, Barnes DE (2007) Trex1 exonuclease degrades ssDNA to prevent chronic checkpoint activation and autoimmune disease. *Cell* 131: 873–886
28. Toledo-Arana A, Dussurget O, Nikitas G, Sesto N, Guet-Revillet H, Bales-trino D, Loh E, Gripenland J, Tiensuu T, Vaitkevicius K et al (2009) The *Listeria* transcriptional landscape from saprophytism to virulence. *Nature* 459: 950–956
29. Davison AJ (2011) Evolution of sexually transmitted and sexually transmissible human herpesviruses. *Ann N Y Acad Sci* 1230: E37–E49
30. Li X, Shu C, Yi G, Chaton CT, Shelton CL, Diao J, Zuo X, Kao CC, Herr AB, Li P (2013) Cyclic GMP-AMP synthase is activated by double-stranded DNA-induced oligomerization. *Immunity* 39: 1019–1031
31. Morrone SR, Matyszewski M, Yu X, Delannoy M, Egelman EH, Sohn J (2015) Assembly-driven activation of the AIM2 foreign-dsDNA sensor provides a polymerization template for downstream ASC. *Nat Commun* 6: 7827
32. Kato H, Takeuchi O, Mikamo-Sato E, Hirai R, Kawai T, Matsushita K, Hiiragi A, Dermody TS, Fujita T, Akira S (2008) Length-dependent recognition of double-stranded ribonucleic acids by retinoic acid-inducible gene-I and melanoma differentiation-associated gene 5. *J Exp Med* 205: 1601–1610
33. Peisley A, Lin C, Wu B, Orme-Johnson M, Liu M, Walz T, Hur S (2011) Cooperative assembly and dynamic disassembly of MDA5 filaments for viral dsRNA recognition. *Proc Natl Acad Sci USA* 108: 21010–21015
34. Berke IC, Yu X, Modis Y, Egelman EH (2012) MDA5 assembles into a polar helical filament on dsRNA. *Proc Natl Acad Sci USA* 109: 18437–18441
35. Zhang X, Wu J, Du F, Xu H, Sun L, Chen Z, Brautigam CA, Zhang X, Chen ZJ (2014) The cytosolic DNA sensor cGAS forms an oligomeric complex with DNA and undergoes switch-like conformational changes in the activation loop. *Cell Rep* 6: 421–430
36. Kranzusch PJ, Vance RE (2013) cGAS dimerization entangles DNA recognition. *Immunity* 39: 992–994
37. Ibsen MS, Gad HH, Thavachelvam K, Boesen T, Despres P, Hartmann R (2014) The 2'-5'-oligoadenylate synthetase 3 enzyme potentially synthesizes the 2'-5'-oligoadenylates required for RNase L activation. *J Virol* 88: 14222–14231